Effects of notches on the order of flux-closure state formation in bi-rings by micromagnetic simulation*

He Shu-Ting(何淑婷), Chang Shuang-Quan(常双全), and Shi Hui-Gang(史慧刚)†

Key Laboratory for Magnetism and Magnetic Materials of the Ministry of Education, Lanzhou University, Lanzhou 730000, *China*

(Received 13 May 2011; revised manuscript received 25 July 2011)

The effects of the number and the location of notches on the formation of flux-closure states in bi-rings with fields applied in the x direction (i.e., along the short axis direction of bi-rings) and y direction (i.e., along the long axis direction of bi-rings) are investigated using micromagnetic simulation. For the bi-rings with one notch and the bi-rings with two notches symmetric about y axis, the order of flux-closure state formation in each ring can be controlled. But the flux-closure state forms simultaneously in each ring for the bi-rings with two notches symmetric about x axis. For the bi-rings with two notches that are symmetric neither about x axis nor about y axis, only one ring can form a flux-closure state in the y-direction field and no flux-closure state can be found in rings in the x-direction field. Therefore, logic states can be defined by controlling the order of flux-closure state formation, which can be utilized in future logic devices.

Keywords: notch(es), the order flux-closure state formation, micromagnetic simulation

PACS: 75.70.Kw, 75.78.Cd, 75.40.Mg **DOI:** 10.1088/1674-1056/20/12/127503

1. Introduction

Nanorings have attracted much attention and have become a promising candidate in data storage application.[1−3] This structure can lead to flux-closure states, without any stray field.[4,5] The chirality of the flux-closure state (clockwise or anticlockwise) can be considered as an information carrier,[6,7] such as high-density storages and magnetic random access memories.[8−10]Arrays of rings have also been studied. Welp *et al.*[11] studied the magnetization behaviour of arrays of coupled Co rings. A magnetic force microscopy image measured by Hirohata *et al.*[12] demonstrated that the ring chain showed flux-closure states in the remanent state. However, magnetostatic interactions and exchange coupling between rings can have an important effect on the magnetic state and reversal process.[5,13] Ren *et al.*[13] investigated the effect of the coupling between bi-rings on their magnetic states. However, the influence of notch(es) on flux-closure states in bi-rings has not yet been explored. For the memory application, the size and the position of memory bits are determined by the notch.[14,15] The notch can control domain wall pinning, thereby allowing some fundamental properties of domain walls to be determined.[16]

In the present work, we study the effects of the number and location of the notches on the order of flux-closure state formation in each ring for overlapping bi-rings with fields applied in the x direction (H_x) and in the y direction (H_y). This structure is of interest because it can create multiple storage states in one physical bit, and it is one possible way to overcome the difficulty of the superparamagnetic limit to magnetic storage density.[17] In this case the multiple stable magnetic states may generate novel properties as recently envisioned in quantum cellular automata.[18] Furthermore, the order of flux-closure state formation in each ring for bi-rings is of interest due to the potential application in logic devices, such as temporal logic devices, sequence pulse generators, etc. In certain devices it can be used to control the order which is set up in advance.

2. Simulation details

All micromagnetic simulations were performed using the three-dimensional (3D) object oriented micromagnetic framework (OOMMF).[19] The mechanism of domain wall motion has been de-

*Project supported by the National Natural Science Foundation of China (Grant No. 50801033).

†Corresponding author. E-mail: shihuig@lzu.edu.cn

© 2011 Chinese Physical Society and IOP Publishing Ltd

scribed theoretically by the Landau–Lifshitz–Gilbert equation[20,21] of magnetization dynamics as

$$\frac{\partial \boldsymbol{M}}{\partial t} = -|\gamma|\,\boldsymbol{M} \times \boldsymbol{H}_{\text{eff}} + \frac{\alpha}{M_{\text{s}}}\left(\boldsymbol{M} \times \frac{\partial \boldsymbol{M}}{\partial t}\right), \quad (1)$$

where $\boldsymbol{M}$ is the magnetization distribution, $\boldsymbol{H}_{\text{eff}}$ is the effective field, M_{s} is the saturation magnetization and $|\gamma| = 2.211 \times 10^5$ (rad/s)/(A/m) is the gyromagnetic ratio. The magnetic parameters for the $Ni_{80}Fe_{20}$ bi-rings used in the present study were as follows: saturation magnetization $M_{\text{s}} = 8.6 \times 10^5$ A/m, exchange constant $A = 1.3 \times 10^{-11}$ J/m and crystalline anisotropy constant $K = 0$. The cell size was set to be 10 nm. Reducing the cell size to 5 nm did not significantly change the results. To reduce the computation time, a damping coefficient $\alpha = 0.5$ was used.[22,23] In order to compare with the results of bi-rings without notches in Ref. [13], we studied bi-rings with one notch and two notches separately. Bi-rings are 50 nm in thickness, 1.2 μm in outer diameter, and 600 nm in inner diameter, and the outer diameter of one ring touches the inner diameter of the other ring, forming a figure 8 shape in this paper (as depicted in Fig. 1). The equilateral triangle notch depth is about 50% of the width of each ring. One ramping magnetic field from −5000 Oe (1 Oe = 79.5775 A/m) to 5000 Oe was applied in the x direction and the other one from −8000 Oe to 8000 Oe was applied in the y direction in all micromagnetic simulations.

3. Results and discussion

Figure 1(a) shows the magnetic hysteresis loop of bi-rings with a notch for an applied H_x field. Insets show its magnetic configurations, corresponding to the labels A, B, C, and D in different regions of the hysteresis loop. All rings exhibit a single domain at positive saturation and all spins are aligned to the external field. When the field is relaxed, each ring exhibits the onion state with two transverse domain walls (A). On further reducing the field, the formation and the motion of vortices in each ring (A1–B) can be seen. Then the vortex which is located below the notch moves to the overlapping region of the rings. The clockwise flux-closure state is formed in the top ring at 50 Oe (C), but it appears in the bottom ring until at 0 Oe (D) with a small vortex present in the overlapping region. With the increase of reversed field, the vortex–to–reverse onion transition comes into being. The V^+–V^- structure is formed at the nucleation site as shown in the circle in A1. The V^+–V^- annihilation process can generate the spin-wave.[5] Therefore, it can be regarded as the source for spin-waves for use in logical circuits.[16,24]

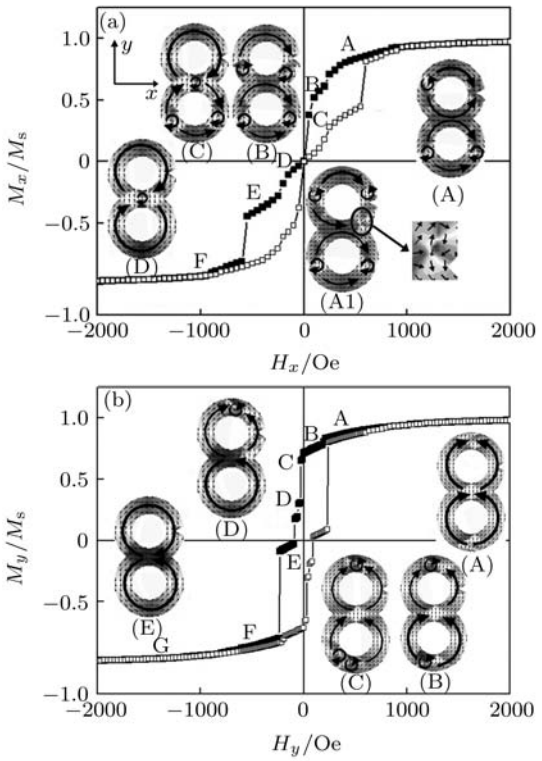


Fig. 1. (a) Magnetic hysteresis loop of bi-rings with a notch for an applied H_x field. Insets show the corresponding magnetic configurations in different regions of the hysteresis loop with the coordinate system used in the text marked out. A1 is a special magnetic configuration between A and B. Vortex (V^+) and antivortex (V^-) structures are both shown in the circle. (b) Magnetic hysteresis loop of bi-rings with a notch for applied H_y field. In this paper, the solid square curves and the open square curves denote hysteresis loops for the bi-rings applied the filed from positive saturation to negative saturation and from negative saturation to positive saturation, respectively.

Figure 1(b) shows the magnetic hysteresis loop of bi-rings with a notch for an applied H_y field. As shown in the initial magnetization configurations A–C, the nucleation and the annihilation of magnetic vortices can be observed in all rings as the field relaxes from positive saturation. At a reverse field of −36 Oe, the bottom ring forms a counterclockwise flux-closure state (D). Between −96 Oe and −228 Oe, the top ring forms a clockwise flux-closure state after nucleation and annihilation of vortex, and there is no domain wall in the overlapping region (E).

So the order of flux-closure state formation can be controlled by adding a notch into bi-rings, regardless of whether an H_x or H_y field is applied. At the same time a pair of V^+– V^- are generated in the nucleation process in an H_x field.

Figures 2(a) and 2(b) show the magnetic hysteresis loops of bi-rings with two notches symmetric about y axis for applied H_x and H_y fields. In Fig. 2(a), in a range between 350 Oe and 38 Oe (B–B1), the propagation of magnetic vortices can be observed in the top ring, but vortices in bottom ring are pinned by notches. A counterclockwise flux-closure state traces around the top ring at 0 Oe (C) first. On further increasing the reverse field, vortices in the bottom ring have enough energy to depin and annihilate. The bottom ring forms a flux-closure state at −100 Oe. So the same chirality of the flux-closure state can emerge in each ring and a small vortex is present in the overlapping region between −100 Oe and −200 Oe (D). Increasing the negative field, the flux-closure state in the top ring is broken first (E). For higher field, all rings exhibit a reverse onion state. The V^+–V^-–V^+ configuration is generated on the top of the top ring as shown in the circle in B1.

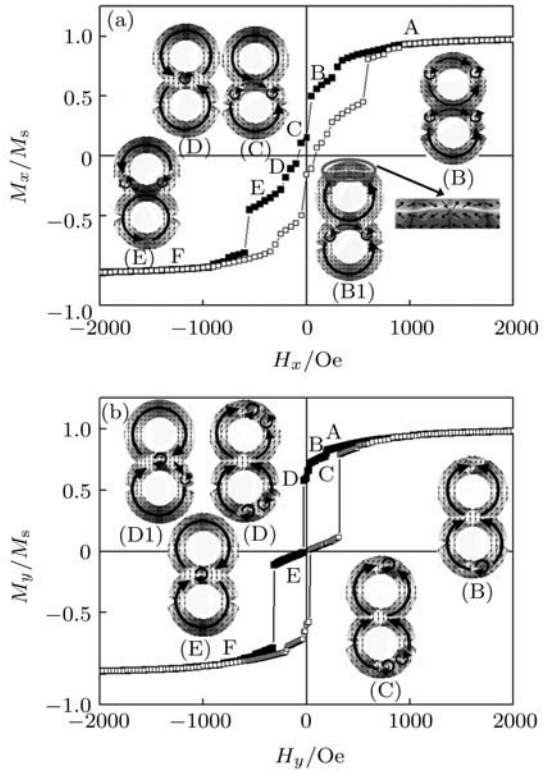


Fig. 2. (a) Magnetic hysteresis loop of bi-rings with two notches symmetric about y axis for an applied H_x field. Insets show the corresponding magnetic configurations in the different regions of the hysteresis loop. The V^+–V^-–V^+ configuration is shown in the circle. B1 is a special magnetic configuration between B and C. (b) Magnetic hysteresis loop of bi-rings with two notches symmetric about y axis for applied H_y field. D1 is a special magnetic configuration between D and E.

For bi-rings with two notches symmetric about y axis in an H_y field, the magnetic hysteresis loop (see Fig. 2(b)) shows a two-step switching with the two switching fields $H_{s1} = -24$ Oe and $H_{s2} = -312$ Oe. Between the onion-to-vortex state transitions, there exist three small steps resulting from the nucleation of magnetic vortices (B–D, see insets) in each ring. The top ring forms a clockwise flux-closure state firstly (D1). The flux-closure state of the bottom ring has the same chirality as that of the top ring, and a small vortex is present in the overlapping region (E) until at −36 Oe.

For bi-rings with two notches symmetric about the y axis, the flux-closure state forms in the top ring first no matter whether an H_x or H_y field is applied. Therefore, the forming order of the flux-closure states can also be controlled by adding two notches symmetric about y axis into bi-rings. The V^+–V^-–V^+ configuration appears in the nucleation process in an H_x field.

Figure 3(a) shows the magnetic hysteresis loop of bi-rings with two notches symmetric about the x axis for an H_x field. Magnetic vortices nucleate and move in each ring between 350 Oe and 59 Oe (B–C2) and then annihilate simultaneously at 0 Oe (D). Therefore, all rings present counterclockwise flux-closure states with a small vortex present in the overlapping region. Each ring exhibits a reverse onion state in higher field values. The V^+–V^-–V^+ structure generates on the top part of the top ring as shown in the circle in C1.

Figure 3(b) shows the magnetic hysteresis loop for bi-rings with two notches symmetric about x axis in an H_y field. Magnetic vortices in bi-rings are not trapped by each notch (B–C1) and annihilate simultaneously. An overall flux-closure state encircles the two rings with a small vortex present in the overlapping region at −72 Oe (D). A pair of V^+–V^- generates on the left part of the top ring as shown in the circle in C1.

For the bi-rings with two notches symmetric about the x axis, the flux-closure state forms simultaneously in each ring no matter whether an H_x or H_y field is applied. That is to say, the order of forming flux-closure states in each ring cannot be controlled. Furthermore, V^+–V^-–V^+ and V^+–V^- configurations can be seen in the nucleation process in H_x and H_y fields, respectively.

Figures 4(a) and 4(b) show the magnetic hysteresis loops of bi-rings with two notches symmetric neither about the x axis nor about y axis for applied H_x and H_y fields, respectively.

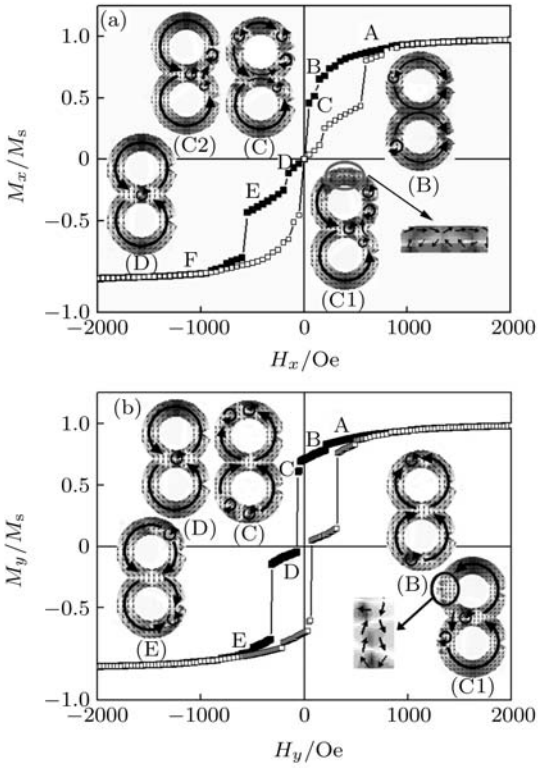


Fig. 3. (a) Magnetic hysteresis loop for bi-rings with two notches symmetric about the x axis for an applied H_x field. Insets show the corresponding magnetic configurations in different regions of the hysteresis loop. The V^+–V^-–V^+ configuration is shown in the circle. C1 and C2 are special magnetic configurations between C and D. (b) Magnetic hysteresis loop of bi-rings with two notches symmetric about the x axis for an applied H_y field. The V^+–V^- configuration is shown in the circle. C1 is a special magnetic configuration between C and D.

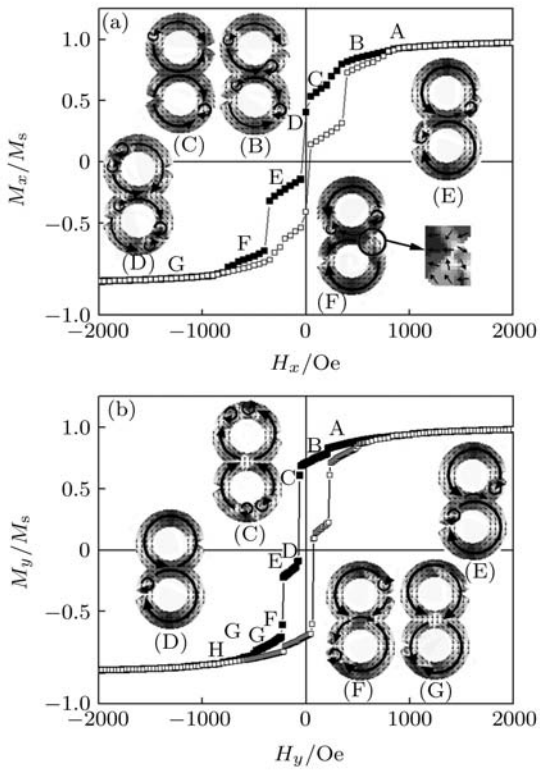


Fig. 4. (a) Magnetic hysteresis loop for bi-rings with two notches symmetric neither about x axis nor about y axis. Insets show the corresponding magnetic configurations in different regions of the hysteresis loop. The V^+–V^- configuration is shown in the circle. (b) Magnetic hysteresis loop for bi-rings with two notches symmetric neither about x axis nor about y axis. Insets show the corresponding magnetic configurations in different regions of the hysteresis loop.

When relaxing the H_x field, the nucleation and the motion of magnetic vortices (B–D) are observed in the onion-to-vortex state transition as shown in the insets in Fig. 4(a). Flux-closure states can be obtained around the main part of each ring, while two vortices are pinned by notches at −50 Oe (E). However, an overall flux-closure state cannot be observed in each ring at higher reversed field and all rings display opposite onion states finally. At −400 Oe, a pair of V^+–V^- is generated on the right side of the overlapping region as shown in the circle in F. Figure 4(b) shows a similar reversal mechanism in the H_y field, but a counterclockwise flux-closure state appears only in the top ring at −72 Oe (D). With increasing negative field, a vortex arises around the notch in the top ring and no flux-closure state can be found in the bottom ring (E). For the higher field values, all rings exhibit an oppose onion state.

For the bi-rings with two notches symmetric neither about x axis nor about y axis, no flux-closure state can be formed in each ring for an applied H_x field, only one ring can form a flux-closure state for an applied H_y field.

4. Conclusions

The effects of the number and the location of notches on the formation of flux-closure states in $Ni_{80}Fe_{20}$ bi-ring are investigated using micromagnetic simulation. It is found that the order of flux-closure state formation in each ring can be controlled by adding one notch and two notches symmetrically about y axis into bi-rings separately. However, for the bi-rings with two notches symmetric about x axis, the flux-closure state forms simultaneously in each ring. For the bi-rings with two notches symmetric neither about x axis nor about y axis, only one ring can form flux-closure state for an applied H_y field but no flux-closure state can be found in each ring for an applied

H_x field. Some antivortices are also generated at nucleation sites, forming V^+–V^-, V^+–V^-–V^+ configurations. Hence, logic states can be defined and possibly utilized in future logic devices by controlling the order of forming flux-closure states.

Acknowledgment

We are grateful to the High Performance Computing Centre at Lanzhou University for the support.

References

[1] Lai M F, Liao C N, San Z H, Lee C P, Hsieh Y P and Ho T F 2008 *J. Appl. Phys.* **103** 07C517

[2] Wen Z C, Wei H X and Han X F 2007 *Appl. Phys. Lett.* **91** 122511

[3] Han X F, Wen Z C and Wei H X 2008 *J. Appl. Phys.* **103** 07E933

[4] Wang J B, Zhang B, Liu Q F, Ren Y and Liu R L 2009 *J. Appl. Phys.* **105** 083908

[5] Rose V, Buchanan K, Chung S H, Grimsditch M, Metlushko V, Hoffmann A, Novosad V, Bader S D and Ibach H 2006 *Phys. Rev.* B **73** 094442

[6] van Waeyenberge B, Puzic A, Stoll H, Chou K W, Tyliszczak T, Hertel R, Fähnle M, Brück H, Rott K, Reiss G, Neudecker I, Weiss D, Back C H and Schütz G 2006 *Nature* **444** 461

[7] Jin W and Liu Y W 2010 *Chin. Phys.* B **19** 037001

[8] Zhu J G, Zheng Y and Prinz G A 2000 *J. Appl. Phys.* **87** 6668

[9] Zheng Y K, Wu Y H, Li K B, Qiu J J, Shen Y T, An L H, Guo Z B, Han G C, Luo P, You D and Liu Z Y 2003 *J. Appl. Phys.* **93** 7307

[10] Han X F, Wei H X, Peng Z L, Yang H D, Feng J F, Du G X, Sun Z B, Jiang L X, Qin Q H, Ma M, Wang Y, Wen Z C, Liu D P and Zhan W S 2007 *J. Mater. Sci. Technol.* **23** 304

[11] Welp U, Vlasko-Vlasov V K, Hiller J M and Zaluzec N J 2003 *Phys. Rev.* B **68** 054408

[12] Hirohata A, Yao C C, Leung H T, Xu Y B, Guertler C M and Bland J A C 2000 *IEEE Trans. Magn.* **36** 3068

[13] Ren Y, Jain S, Adeyeye A O and Ross C A 2010 *New. J. Phys.* **12** 093003

[14] Huang S H and Lai C H 2009 *Appl. Phys. Lett.* **95** 032505

[15] Choe S B 2008 *J. Magn. Magn. Mater.* **320** 1112

[16] Bogart L K, Eastwood D S and Atkinson D 2008 *J. Appl. Phys.* **104** 033904

[17] Chang Y C, Chang C C, Chang I, Wu J C, Wei Z H, Lai M F and Chang C R 2006 *J. Appl. Phys.* **99** 08B710

[18] Cowburn R P and Welland M E 2000 *Science* **287** 1466

[19] Donahue M J and Porter D G 2009 *OOMMF User's Guide*, Version 1.2a3 (http://math.nist.gov/oommf)

[20] Sun Z Z and Schlieman J 2010 *Phys. Rev. Lett.* **104** 037206

[21] Chen W B, Han M G, Zhou H, Ou Y and Deng L J 2010 *Chin. Phys.* B **19** 087502

[22] Hayward T J, Moore T A, Tse D H Y, Bland J A C, Castaño F J and Ross C A 2005 *Phys. Rev.* B **72** 184430

[23] Wang X H Goolaup S and Lew W S 2010 *Appl. Phys. Lett.* **97** 142504

[24] Gliga S, Yan M, Hertel R and Schneider C M 2008 *Phys. Rev.* B **77** 060404